N83-24541

THE
BENDIX
CORPORATION

GUIDANCE
SYSTEMS
DIVISION

TETERBORO
NEW JERSEY   07608

MODULAR DESIGN
ATTITUDE CONTROL
SYSTEM

FINAL REPORT
18 MARCH 1983

PREPARED FOR:

GEORGE C. MARSHALL
SPACE FLIGHT CENTER
HUNTSVILLE,ALABAMA

NASA CONTRACT NO.
NAS8-33979
EXHIBIT B

OCTOBER 16, 1981
        to
OCTOBER 31, 1982

Bendix **Guidance Systems Division**

THE
BENDIX
CORPORATION

GUIDANCE
SYSTEMS
DIVISION

TETERBORO
NEW JERSEY   07608

MODULAR DESIGN
ATTITUDE CONTROL
SYSTEM

FINAL REPORT
18 MARCH 1983

PREPARED FOR:

GEORGE C. MARSHALL
SPACE FLIGHT CENTER
HUNTSVILLE,ALABAMA

NASA CONTRACT NO.
NAS8-33979
EXHIBIT B

OCTOBER 16, 1981
          to
OCTOBER 31, 1982

APPROVED BY:

J. LEVINTHAL
ENGINEERING MANAGER
SYSTEMS DESIGN

PREPARED BY:

F.D. CHICHESTER
TECHNICAL MANAGER

N83-24541

FOREWORD

ABSTRACT

Application of modular control techniques to the attitude
control of a prototype flexible spacecraft and a prototype
flexible space platform was further developed by determining
numerical values for the physical parameters of a four body
approximation of the MSFC/hybrid deployable truss incorporat-
ed in the space platform model, generating sensitivity coef-
ficients for the model of the flexible spacecraft, evaluating
the changes in the digital computer simulation of the flexi-
ble spacecraft resulting from the addition of another rigid
body to the model and comparing attitude control effective-
ness with actuators on more than one rigid body of the model
with that for the case in which the actuators were restricted
to one body.

TABLE OF CONTENTS

LIST OF ILLUSTRATIONS

LIST OF TABLES

SECTION 1

1.0   INTRODUCTION

This report is submitted in compliance with the Scope of Work under contract NAS8-33979. The period of performance covered by the contract is from October 15, 1981 to October 31, 1982. The submission and approval of this report constitute the successful completion of the "Exhibit B" portion of the contract.

This report is a sequel to three others, two of them previously submitted under a different contract number. The two prior reports, under a different contract number, references (1-1) and (1-2), were submitted in October 1978 and September, 1979 and covered the periods from July 27, 1977 to July 27, 1978 and from August 26, 1978 to August 26, 1979, respectively, in compliance with "Exhibit A" of contract NAS8-32660.

The prior report under contract NAS-33979, reference (1-3), was submitted on March 8, 1982 and covered the period from August 15, 1980 to October 15, 1981 in compliance with "Exhibit A" of the contract.

1.1   OBJECTIVES

The sections that follow summarize the effort expended on the Modular Design Attitude Control System Study contract. The overall objective of the study was to further develop a new approach to applying attitude control to mathematical models of the rotational dynamics of a representative flexible spacecraft and of a representative space platform incorporating both the flexible spacecraft and a deployable truss.

More specifically, to complete the digital computer simulation of the ten body model of the prototype flexible space platform initiated during the previous reporting period, it was necessary to determine numerical values for the physical parameters of the four body approximation of the MSFC/hybrid deployable truss that had been developed algebraically. Additional specific objectives included development of numerical values for the relative sensitivity of the state variables of the flexible spacecraft model to changes in the numerical values of its physical parameters, evaluation of changes in the digital computer simulation of the model required to accommodate addition of another rigid body and comparison of attitude control effectiveness between the case in which actuators were distributed over more than one rigid body of the model and the case in which they were restricted to one body.

1.2   SCOPE

Study effort was concentrated in five main areas:

1. Development of a dynamically equivalent four body approximation of the NASTRAN finite element model supplied for the MSFC/hybrid deployable truss to support the digital computer simulation of the ten body model of the flexible space platform that incorporates the four body truss model.

2. Generation of coefficients for sensitivity of state variables of the linearized model of the three axes rotational dynamics of the prototype flexible spacecraft with respect to the model's parameters.

3. Evaluation of software changes required to accommodate addition of another rigid body to the five body model of the rotational dynamics of the prototype flexible spacecraft.

4. Comparison of effectiveness of attitude control for actuators on two bodies of the six body model of the prototype flexible space platform with that for actuators restricted to one body of the same model.

1.3 GENERAL

This report is comprised of six sections. Section 2 describes the determination of the numerical values of the parameters of the four body model of the MSFC/hybrid deployable truss in such a way that five modes of its rotational dynamics closely matched those of NASTRAN finite element model described in Ivey (1-4). Section 3 describes the generation of coefficients of the sensitivity of the state variables to changes in the parameters of the linearized five body model of the rotational dynamics of the prototype flexible spacecraft. Section 4 presents an evaluation of the changes in the computer simulation of the five body model of the prototype flexible spacecraft required to accommodate the addition of another rigid body to the model. Section 5 presents a comparison of the effectiveness of modular attitude control for actuators on two bodies of the six body model of the prototype space platform with that for actuators restricted to one body of the same model. Section 6 lists a number of conclusions and recommendations drawn from the results of the tasks described above. References are listed at the end of each section.

The original RFQ requested that the International System of units (designated as SI) be used in the program and in any reporting. Torques, moments, angular momentum, moments of inertia and distances, however, are stated in English units since this was the system of units used in presenting all of the vehicle data in the RFQ and the truss data in Ivey (1-4).

1.4 REFERENCES

1-1 Guidance Systems Division, The Bendix Corporation, "Space Construction Base Control System", Final Report, Contract NAS8-32660 for George C. Marshall Space Flight Center, October 27, 1978.

1-2 Guidance Systems Division, The Bendix Corporation, "Space Construction Base Control System", Final Report, Contract NAS8-32660 for George C. Marshall Space Flight Center, September 1, 1979.

1-3 Guidance Systems Division, The Bendix Corporation, "Modular Design Attitude Control System", Final Report, Contract NAS8-33979 for George C. Marshall Space Flight Center, March 8, 1982.

1-4 Ivey, Wayne, "Vibration Analysis of the MSFC/Hybrid Deployable Truss", Marshall Space Flight Center memorandum, June 26, 1980.

SECTION 2

2.0 APPROXIMATING A NASTRAN FINITE ELEMENT MODEL OF THE HYBRID DEPLOYABLE TRUSS BY A FOUR BODY MODEL

2.1 INTRODUCTION

In Chichester (2-1), a prototype flexible spacecraft comprised of a rigid central body with two flexible solar wings was approximated by an assembly of five rigid bodies interconnected by a spring hinge suspension shown in Figure 2-1. The resulting linearized model of the rotational dynamics of the spacecraft was written in state variable form to facilitate the application of multilevel attitude control. In later work, Chichester (2-2), this prototype flexible spacecraft was connected to another spacecraft via a hybrid deployable truss to form a flexible space platform. This flexible space platform was approximated by the assembly of ten rigid bodies interconnected by a spring hinge suspension, depicted in Figure 2-2, under the assumptions that the second spacecraft could be approximated by a single rigid body and the truss could be approximated by four rigid bodies serially connected by a spring hinge suspension. The rotational dynamics of the MSFC/hybrid deployable truss were presented in Ivey (2-3) in terms of a NASTRAN finite element analysis of the response of the truss to perturbations while it was in a cantilever configuration.

The work reported in the present section was directed toward approximating the NASTRAN model of the truss with a model consisting of four bodies serially connected by a spring hinge suspension. This approximation was effected by application of the following procedure:

2-1

THREE DEGREE OF FREEDOM HINGES
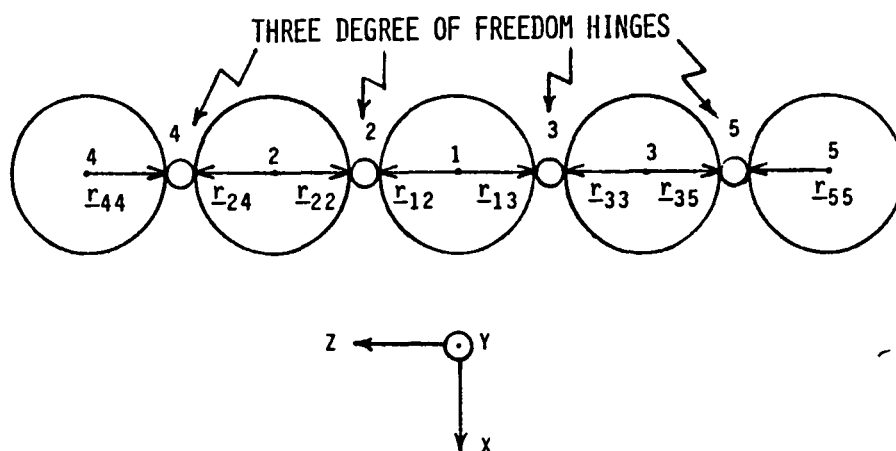
FIGURE 2-1.

TOPOLOGICAL DIAGRAM OF FIVE BODY
APPROXIMATION OF A PROTOTYPE FLEXIBLE SPACECRAFT
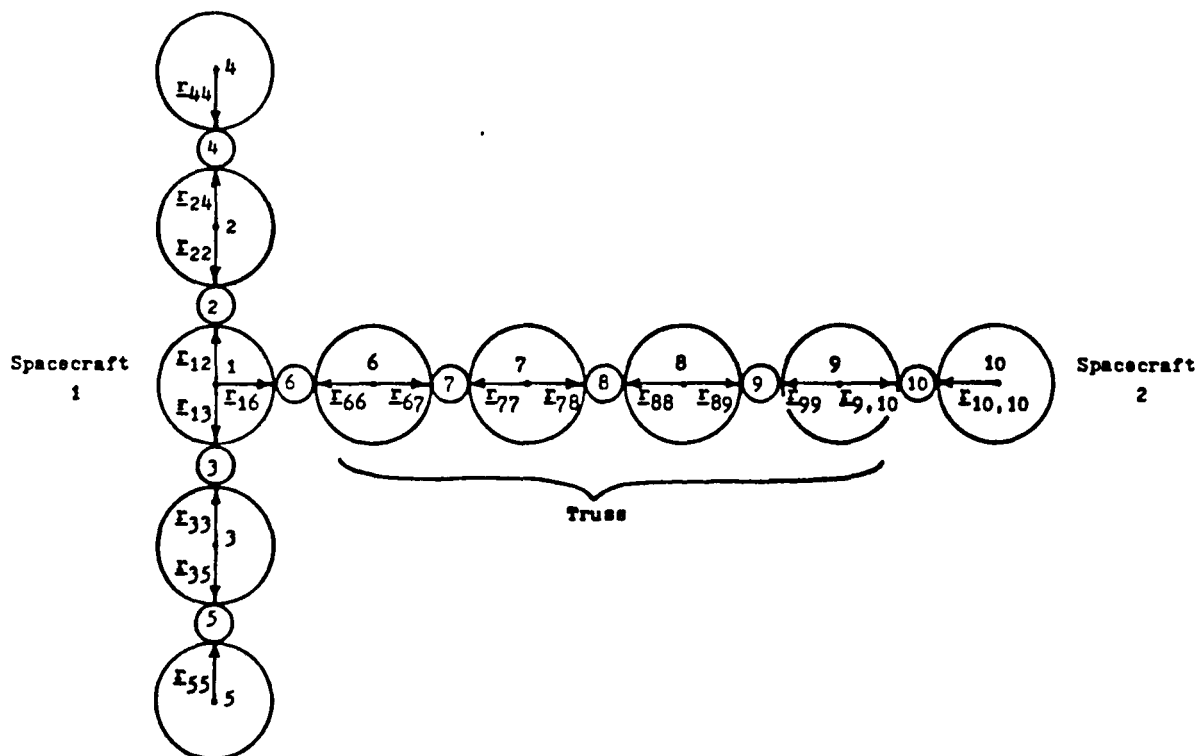
FIGURE 2-2.

TOPOLOGICAL DIAGRAM OF TEN BODY APPROXIMATION

OF TWO SPACECRAFT INTERCONNECTED BY A DEPLOYABLE TRUSS

1. Decompose the truss into four serially connected modules
    determining the total mass and rotational inertias for a
    rigid body with its mass center on the axis of the truss
    for each module.

2. Develop five body cantilever truss model.

3. Develop undamped form of cantilever truss model.

4. Generate spring coefficient values to match eigenvalues
    of undamped five body cantilever truss model with those
    of the NASTRAN model.

5. Generate damping coefficients to add n% of critical damp-
    ing to the five body model of the cantilever truss with
    eigenvalues matching those of the NASTRAN model.

2.2   DECOMPOSITION OF TRUSS INTO MODULES

A perspective drawing of the MSFC/hybrid deployable truss
that appeared in Ivey (2-3) is reproduced in Figure 2-3 with
shaded circles representing the locations of the centers of
mass of four 8000 pound payloads rigidly attached to the
fifth and tenth cubic submodules of the truss. The truss and
its payloads were decomposed into two pairs of identical mod-
ules serially connected by three degree of freedom hinges
shown in Figure 2-4. Each module in one pair consists of
only four cubic submodules of the truss. Each module in the
other pair consists of one cubic submodule of the truss with
8000 pound payloads rigidly attached both above and below
it. An equivalent rigid body with its center of mass located
on the centerline of the truss and the same total mass and
rotational inertias was determined for each of the four mod-
ules under the following assumptions:
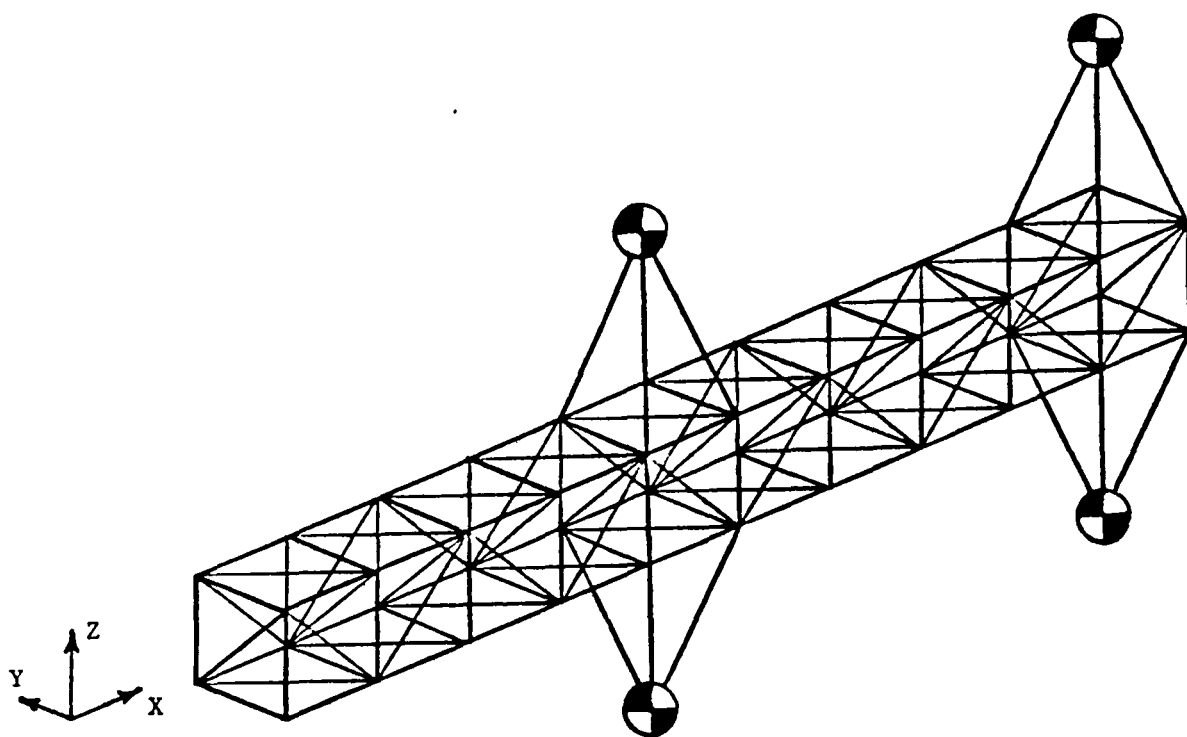
FIGURE 2-3.   PERSPECTIVE VIEW OF HYBRID DEPLOYABLE TRUSS
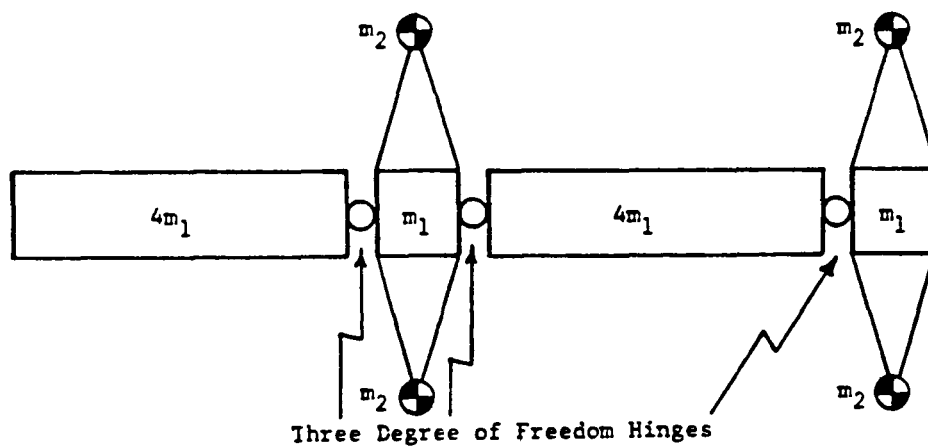
FIGURE 2-4

SIDE VIEW OF MODULES OF DECOMPOSED TRUSS

1. The mass of each cubic truss submodule is uniformly distributed in the cube.

2. The mass of each payload may be represented as a point mass at its center of mass.

Details of the analysis to determine these equivalencies appear in Chichester and Emmanuel (2-4).

The equivalent total masses and rotational inertias for the rigid bodies representing the modules are presented in Table 2-1. The parameters utilized in this table are the following:

m_1 = total mass of cubic submodule of truss

m_2 = total mass of 8000 pound payload

L_1 = 1/2 length of one side of cubic submodule of truss

L_2 = distance of center of mass of payload from nearest face of cubic submodule of truss.

The determination of the total masses and rotational inertias of the equivalent rigid bodies reduced the model of the truss to four rigid bodies with their centers of mass located on the axis of symmetry of the truss serially connected by three degree of freedom hinges with associated rotational spring and damping coefficients.

2.3 DEVELOPMENT OF CANTILEVER TRUSS MODEL

The vibrational modes obtained for the finite element NASTRAN model of the hybrid truss in Ivey (2-3) resulted from perturbing the end of the truss to which the payloads are

TABLE 2-1.

EQUIVALENT TOTAL MASSES AND
ROTATIONAL INERTIAS OF TRUSS MODULES

	MODULES W/O PAYLOAD	MODULES WITH PAYLOAD
Total Mass	$4m_1$	$2m_2 + m_1$
I_x	$\frac{8}{3}m_1L_1^2$	$m_2\left[(L_1 + L_2)^2 + \frac{2m_1}{3m_2}L_1^2\right]$
I_y	$\frac{68}{3}m_1L_1^2$	same as I_x
I_z	same as I_y	$\frac{2}{3}m_1L_1^2$

attached while its unloaded end was attached to a wall in a cantilever configuration. To replicate these conditions, the unloaded end of the four body model of the truss was attached via a three degree of freedom hinge to a fifth body of large mass and rotational inertia with its center of mass close to this hinge. The imposition of these conditions yields responses to displacements of the free end of the truss that very closely approximate cantilever responses according to investigations by Lipski (2-5).

The topological diagram of the five body cantilever truss model is depicted in Figure 2-5 which is of the same form as the one developed for the prototype flexible spacecraft in Chichester (2-1) but with different values for the masses and rotational inertias of the rigid bodies. From equation (19) of Chichester (2-1) the linearized state variable representation of the five body rotational dynamics model of the truss without either external or control torques may be written as follows:

$$\dot{\underline{\omega}} = GLC_s\underline{\omega} + GLK_s\hat{\underline{\alpha}} \qquad (2-1)$$

$$\dot{\hat{\underline{\alpha}}} = K\underline{\omega} \qquad (2-2)$$

where:

$$\underline{\omega} = (\underline{\omega}_1^T, \underline{\omega}_2^T, \ldots, \underline{\omega}_5^T)^T$$

$$\underline{\omega}_1 = (\omega_{ix}, \omega_{iy}, \omega_{iz}) = \text{rate of angular rotation of ith}$$
$$\text{rigid body}$$

$$\hat{\underline{\alpha}} = (\hat{\underline{\alpha}}_1^T, \hat{\underline{\alpha}}_2^T, \ldots, \hat{\underline{\alpha}}_5^T)^T$$

$$\hat{\underline{\alpha}}_1 = \underline{\alpha}_{24} \qquad \hat{\underline{\alpha}}_2 = \underline{\alpha}_{35} \qquad \hat{\underline{\alpha}}_3 = \underline{\alpha}_{12} \qquad \hat{\underline{\alpha}}_4 = \underline{\alpha}_{13} \qquad \hat{\underline{\alpha}}_5 = \underline{\alpha}_1$$
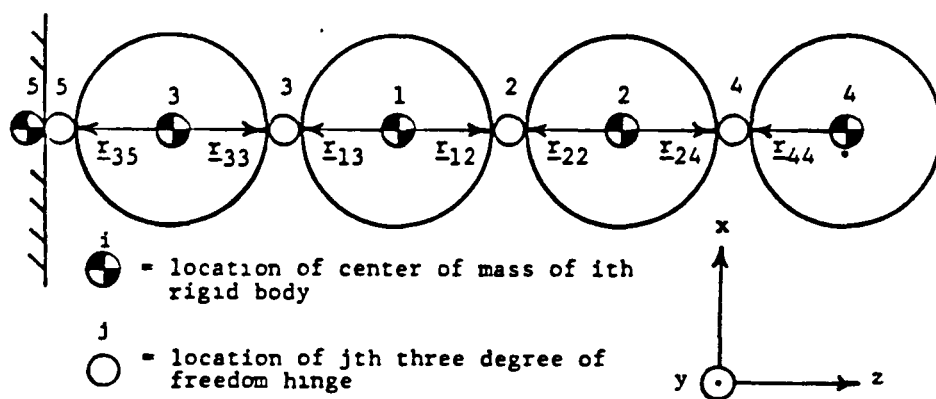
FIGURE 2-5.

FIVE BODY MODEL OF TRUSS IN CANTILEVER CONFIGURATION

$$\underline{\alpha}_1 = (\phi_1, \theta_1, \psi_1)^T$$

$$\underline{\alpha}_{ij} = (\phi_{ij}, \theta_{ij}, \psi_{ij})^T$$

ϕ_1, θ_1, ψ_1 = inertially referenced Euler angles of body 1

$\phi_{ij}, \theta_{ij}, \psi_{ij}$ = relative Euler angles of body j with respect to body i

G, L, C_s, K_s, K = coefficient matrices defined in Chichester (2-1)

2.4 DEVELOPMENT OF UNDAMPED FORM OF THE CANTILEVER TRUSS MODEL

With the mass and rotational inertias determined for each rigid body in the five body model of the cantilever truss the values of the spring and damping coefficients associated with the three degree of freedom hinges were determined in such a way that the first several vibrational modes of the five body model closely matched those of the NASTRAN finite element model. The basis for this matching was the adjustment of these parameters until the corresponding eigenvalues of the two models were closely matched. To this end, the five body cantilever truss model was transformed to its undamped form. This was accomplished as follows. Differentiating equation (2-2) with respect to time yields:

$$\hat{\ddot{\underline{\alpha}}} = K\dot{\underline{\omega}} \tag{2-3}$$

Premultiplying both sides of equation (2-2) by K^{-1} yields:

$$\underline{\omega} = K^{-1}\hat{\dot{\underline{\alpha}}} \tag{2-4}$$

Substitution of equations (2-3) and (2-4) into (2-1) yields the basic equation for the unforced system in terms of Euler angles.

$$\underline{\ddot{\hat{\alpha}}} = KGLC_sK^{-1}\underline{\dot{\hat{\alpha}}} + KGLK_s\underline{\hat{\alpha}} \qquad (2-5)$$

The undamped form of the unforced system model was written by omitting the term including $\underline{\dot{\hat{\alpha}}}$:

$$\underline{\ddot{\hat{\alpha}}} - KGLK_s\underline{\hat{\alpha}} = \underline{0} \qquad (2-6)$$

The undamped natural frequencies corresponding to the modes of the system described by equation (2-6) are the square roots of the corresponding eigenvalues of the system as shown in Lipski (2-5).

The above undamped model was partitioned according to spatial axis as follows:

$$\underline{\ddot{\phi}} - (KGLK_s)_x\underline{\phi} = \underline{0}$$

$$\underline{\ddot{\theta}} - (KGLK_s)_y\underline{\theta} = \underline{0} \qquad (2-7)$$

$$\underline{\ddot{\psi}} - (KGLK_s)_z\underline{\psi} = \underline{0}$$

where:

$$\underline{\phi} = (\phi_{24},\ \phi_{35},\ \phi_{12},\ \phi_{13},\ \phi_1)^T$$

$$\underline{\theta} = (\theta_{24},\ \theta_{35},\ \theta_{12},\ \theta_{13},\ \theta_1)^T$$

$$\underline{\psi} = (\psi_{24},\ \psi_{35},\ \psi_{12},\ \psi_{13},\ \psi_1)^T$$

$$KGLK_s = \begin{bmatrix} (KGLK_s)_x & [0] & [0] \\ [0] & (KGLK_s)_y & [0] \\ [0] & [0] & (KGLK_s)_z \end{bmatrix}$$

$\underline{0}$ = null vector of dimension 5

[0] = 5 x 5 null matrix

2.5 GENERATION OF SPRING COEFFICIENTS TO MATCH EIGENVALUES OF UNDAMPED MODELS

The undamped five body cantilever truss model was simulated on a digital computer to generate values of the spring coefficients that correspond to close matching between eigenvalues of the five body model and those of the NASTRAN finite element model. Since the five body cantilever truss model was based upon decomposition of the truss itself into four modules, matching was sought for just five of the eigenvalues corresponding to two vibrational modes about each of two of the spatial axes and one about the third axis. To attain this matching an algorithm utilizing a steepest descent or gradient method was programmed to systematically vary the values of the 12 spring coefficients until the five eigenvalues of the five body model of the undamped cantilever truss were closely matched with those of the NASTRAN model.

Implementation of this approach resulted in matches between corresponding eigenvalues of the two truss models with an accuracy of three decimal digits. The corresponding values of the spring coefficients are displayed in Table 2-2.

2-13

TABLE 2-2.

SPRING COEFFICIENTS

CORRESPONDING TO MATCHING OF FIVE EIGENVALUES

$$k_{sij} \left[\text{ft.-lb./rad.} \right]$$

Spatial Axis Components	k_{s12}	k_{s13}	k_{s24}	k_{s35}
x	5.653×10^2	5.671×10^2	1.227×10^2	1.162×10^2
y	2.327×10^6	1.838×10^5	2.390×10^5	1.191×10^5
z	1.171×10^2	3.362×10^2	1.215×10^4	6.639×10^3

2.6 DETERMINATION OF DAMPING COEFFICIENTS CORRESPONDING TO n% OF CRITICAL DAMPING

The vector matrix equation representing the damped unforced five body model of the cantilever truss, equation (2-5), was partitioned according to spatial axis by the same procedure as was utilized for the spatial partioning of the undamped model. The resulting set of three vector matrix equations was then expanded to a set of 12 scalar equations by writing the first four scalar components of each vector matrix equation corresponding to a spatial axis. Each of these scalar equations corresponded to one of the relative Euler angles, ϕ_{ij} for the x axis, θ_{ij} for the y axis, and ψ_{ij} for the z axis, where $ij = 24, 35, 12, 13$. In general, the equation for each relative Euler angle contained terms representing coupling with the other three relative Euler angles about the same axis. The coupling terms were ignored and the Laplace transform was applied to the resulting set of decoupled scalar equations. Since, in general, $\Phi_{ij}(s)$, $\theta_{ij}(s)$ and $\Psi_{ij}(s) \neq 0$, their coefficients in the frequency domain must then be equal to zero resulting in the following set of 24 equations.

x axis: $s^2 + b_{ijx}s + c_{ijx} = 0$ $\qquad \dfrac{b_{ijx}}{c_{ijx}} = \dfrac{c_{sijx}}{k_{sijx}}$

y axis: $s^2 + b_{ijy}s + c_{ijy} = 0$ $\qquad \dfrac{b_{ijy}}{c_{ijy}} = \dfrac{c_{sijy}}{k_{sijy}}$ $\qquad$ (2-8)

z axis: $s^2 + b_{ijz}s + c_{ijz} = 0$ $\qquad \dfrac{b_{ijz}}{c_{ijz}} = \dfrac{c_{sijz}}{k_{sijz}}$

where:

$\qquad ij = 24, 35, 12, 13$

For critical damping, the discriminant of each of the above quadratic equations equals zero. Applying this condition led to the following set of equations for the damping coefficients in terms of the spring coefficients corresponding to n% of critical damping. (Damping coefficient values obtained for n = 1 appear in Table 2-3.)

$$c_{sijx} = .02n(c_{ijx})^{-\frac{1}{2}} k_{sijx}$$

$$c_{sijy} = .02n(c_{ijy})^{-\frac{1}{2}} k_{sijy} \qquad\qquad (2-9)$$

$$c_{sijz} = .02n(c_{ijz})^{-\frac{1}{2}} k_{sijz}$$

Details on the matching of the rotational dynamics of the four body model to those of the NASTRAN model of the truss appear in Chichester and Emmanual (2-6).

TABLE 2-3.

DAMPING COEFFICIENTS CORRESPONDING
TO 1% OF CRITICAL DAMPING WITH MATCHED EIGENVALUES

$$c_{sij} \left[\text{ft.-lb /rad /sec.} \right]$$

Spatial Axis Components	c_{s12}	c_{s13}	c_{s24}	c_{s35}
x	1.186	1.137	.4413	5.046
y	$3\ 737 \times 10^3$	1.106×10^3	1.198×10^2	2.629×10^3
z	.5849	.9911	5.958	4.405

2.7 REFERENCES

2-1 Chichester, F.D. "Development of a Three Axis Gauss-Siedel Model of a Flexible Space Vehicle", _Proceedings of the Twelfth Annual Pittsburgh Conference on Modeling and Simulation_, April 1981, University of Pittsburgh, Pittsburgh, Pennsylvania, pp. 1303-1308.

2-2 Chichester, F.D. "Modeling Rotational Dynamics of a Flexible Space Platform for Application of Multilevel Attitude Control", _Proceedings of the 1982 American Control Conference_, June 1982, Arlington, Virginia, pp. 636-642.

2-3 Ivey, Wayne, "Vibration Analysis of the MSFC/Hybrid Deployable Truss", George C. Marshall Space Flight Center (NASA) internal memorandum, June 1980.

2-4 Chichester, F.D., "Modular Design Attitude Control System Final Report", NASA Contract No. NAS 8-33979, Bendix Corporation, Guidance Systems Division, March 8, 1982.

2-5 Lipski, D.B., "Linearized Five Body Truss Model", Bendix ICAT/Simulation Centers Internal Memorandum DBL-12-81-06, December 11, 1981.

2-6 Chichester, F.D. and I.S. Emmanuel, "Approximating a Finite Element Model of a Hybrid Deployable Truss by a Discrete Mass Model", _Proceedings of the Thirteenth Annual Pittsburgh Conference on Modeling and Simulation_, April, 1982, University of Pittsburgh, Pittsburgh, Pennsylvania, pp. 13-18.

SECTION 3

3.0 GENERATING NUMERICAL VALUES FOR SENSITIVITY COEFFICIENTS OF SCALAR STATE VARIABLES WITH RESPECT TO MODEL PARAMETERS

3.1 INTRODUCTION

Earlier work in the application of modular control to flexible spacecraft, Chichester (3-1), (3-2) and (3-3), was predicated upon the assumptions that all of the numerical values of the physical parameters of the model of the flexible spacecraft being controlled were known to sufficient accuracy and were sufficiently time-invariant to support effective attitude control. Since the physical parameters of actual spacecraft rarely satisfy these rather broad assumptions, it is necessary to assess the sensitivity of the time trajectories of the state variables of the rotational model of the flexible spacecraft to small changes in the numerical values of each of these parameters.

The study presented in this section is based upon the linearized state variable model of the rotational dynamics of the five body approximation of the prototype-flexible spacecraft developed in Chichester (3-4) and depicted in Figure 2-1.

The optimal attitude control problem associated with this model may be stated as follows:

Minimize:

$$P = \int_{t_o}^{t_f} (\underline{x}^T Q \underline{x} + \underline{u}^T W_u \underline{u}) dt \qquad (3-1)$$

subject to the linearized state variable (constraint) equation:

$$\dot{\underline{x}} = A\underline{x} + B\underline{u}; \quad t\varepsilon[t_o, t_f] \tag{3-2}$$

where:

$\underline{x} = (\underline{\omega}^T, \hat{\underline{\alpha}}^T)^T$ = state vector of dimension 30

$\underline{\omega} = (\underline{\omega}_1^T, \underline{\omega}_2^T, \ldots, \underline{\omega}_5^T)^T$ = body angular rate vector of dimension 15

$\hat{\underline{\alpha}} = (\underline{\alpha}_{24}^T, \underline{\alpha}_{35}^T, \underline{\alpha}_{12}^T, \underline{\alpha}_{13}^T, \underline{\alpha}_1^T)^T$

$\underline{\omega}_k = (\omega_{kx}, \omega_{ky}, \omega_{kz})^T$ = angular rotation rate of kth body

$\underline{\alpha}_{ij} = (\phi_{ijx}, \theta_{ijy}, \psi_{ijz})^T$

$\phi_{ij}, \theta_{ij}, \psi_{ij}$ = relative Euler angles of body j with respect to body i

ϕ_1, θ_1, ψ_1 = inertially referenced Euler angles of central body (body 1)

Q = state vector error coefficient matrix of dimension 30 × 30

W_u = control vector energy coefficient matrix of dimension r × r (r ≤ 15)

A = state vector coefficient matrix of dimension 30 × 30

B = control vector coefficient matrix of dimension
30 × r

$\underline{u}$ = control vector of dimension r

t_O = initial time

t_f = final time

3.2   PROCEDURE FOLLOWED

1. Express the state vector coefficient matrix, A, and the
    control vector coefficient matrix, B, in the state varia-
    ble linearized model of the rotational dynamics of the
    five body approximation of the prototype flexible space-
    craft in terms of the model parameters p_j, j = 1, 2, ...,
    54 which represent:

    o   five body masses

    o   15 non-zero coefficients of rotational inertia

    o   10 non-zero spatial components of location vectors for
        mass centers of the rigid bodies comprising the model

    o   12 spring coefficients

    o   12 damping coefficients

2. Corresponding to the perturbed value,

$$p'_j = p_j + \Delta p_j, \qquad\qquad (3\text{-}3)$$

    of each model parameter develop a perturbed state varia-
    ble model of the rotational dynamics of the flexible

spacecraft by incorporating the corresponding perturbed coefficient matrices,

$$A' = A\Big|_{p_j \to p_j'} \quad \text{and} \quad B' = B\Big|_{p_j \to p_j'} \tag{3-4}$$

3. Develop the corresponding perturbed optimal attitude control problem for each perturbed model generated in Step 2. For each model parameter perturbation, Δp_j, the corresponding perturbed optimal attitude control problem is expressed as follows:

Minimize:

$$P' = \int_{t_o}^{t_f} [(\underline{x}')^T Q \underline{x}' + (\underline{u}')^T W_u \underline{u}'] dt \tag{3-5}$$

subject to the perturbed linearized state variable (constraint) equation,

$$\dot{\underline{x}}' = A' \underline{x}' + B' \underline{u}'. \tag{3-6}$$

The solution vectors for this control problem are $\underline{x}'(t)$ and $\underline{u}'(t)$ for $t \epsilon [t_o, t_f]$.

4. Simulate each perturbed optimal attitude control problem of Step 3 on a digital computer and obtain the perturbed control vector, response $\underline{u}'(t)$, to a standard initial displacement for each perturbed model parameter, p'_j.

5. Utilize a digital computer simulation of the unperturbed state variable model (with coefficient matrices A and B instead of A' and B', respectively) to generate the time

trajectories of the state vectors, $\underline{x}(t)$, of the unperturbed model to each of the perturbed control vector time trajectories, $\underline{u}'(t)$, generated in Step 4 in conjunction with the same initial displacements. The unperturbed linearized state variable model with the perturbed control vector, $\underline{u}'(t)$, as a forcing function then takes the following form

$$\dot{\underline{x}}'' = A\underline{x}'' + B\underline{u}' \tag{3-7}$$

where $\underline{x}''(t)$ represents the resulting state vector solution for $t \epsilon \lfloor t_o, t_f \rfloor$.

6. Use scalar state responses, $x_i(t)$, of the original model **without any perturbations** in conjunction with the corresponding scalar components of the state vectors obtained in Step 5 to generate the following scalar state perturbations.

$$\Delta x_i(t) = x_i''(t) - x_i(t) \qquad t \epsilon \lfloor t_o, t_f \rfloor \tag{3-8}$$

7. Construct a table of maximum magnitude sensitivity coefficients, S_{ijm}, by utilizing the following definition.

$$S_{ijm} = \frac{\text{Max}}{t \epsilon \lfloor t_o, t_f \rfloor} \left| \frac{\Delta x_i}{\Delta p_j} \right| \tag{3-9}$$

8. Construct a table of "steady state" sensitivity coefficients, S_{ijss}, by using the following relationship

$$S_{ijss} = \frac{\Delta x_i(t_f)}{\Delta p_j} \tag{3-10}$$

3.3 RESULTS

Representative numerical results of the application of the procedure described above are displayed in Tables 3-1 and 3-2 with the entry of largest magnitude in the upper left corner and the remaining entries in descending order across the rows and down the columns. The entries of Table 3-1, the maximum magnitude sensitivity coefficients, S_{ijm}, provide an index to the relative sensitivity of the scalar state variables, x_i, to changes in the numerical values of the model's parameters, p_j, while the controlled system is responding to a disturbance. The entries of Table 3-2, the steady state or final time sensitivity coefficients, S_{ijss}, provide an ordering of the relative sensitivity of the state variables, x_i, to changes in the numerical values of the model's parameters, p_j, when the controlled system is at an equilibrium condition. In both tables the Euler angles ϕ, θ, ψ, represent rotations about the x, y and z spatial axes, respectively, and the double subscript, ij, on the relative Euler angles represents angular displacement of body j with respect to body i.

Comparison of the two tables reveals certain patterns common to the two. For example, the six largest transient sensivity ratios are, in descending order along the first column of entries in Table 3-1,

$$\left|\frac{\Delta\phi_1}{\Delta c_{s_{35}z}}\right|_{max} , \quad \cdots \cdots , \quad \left|\frac{\Delta\phi_1}{\Delta v_{12z}}\right|_{max} * \qquad (3\text{-}11)$$

*v_{ijz} represents the z axis component of the location vector of the jth hinge with respect to the mass center of the ith body.

TABLE 3-1
MAGNITUDE ORDERING OF SENSITIVITY COEFFICIENT MAXIMA

$$\left|\frac{\Delta x_i}{\Delta p_j}\right|_{\max}\ t\ \varepsilon\ [t_o,\ t_f]$$

p_j \ x_i	ϕ_1	ϕ_{24}	θ_1	ψ_{24}	ψ_{35}	ϕ_{35}	ψ_1	ω_{5x}	ω_{4x}
c_{s35z}	4.00	2.64	2.51	2.23	2.23	2.21	1.86	1.81	1.64
c_{s24z}	4.00	2.64	2.51	2.23	2.23	2.21	1.86	1.81	1.64
c_{s13z}	3.58	2.36	2.24	1.99	1.99	1.97	1.66	1.61	1.47
c_{s12z}	3.57	2.36	2.24	1.99	1.99	1.97	1.66	1.61	1.47
v_{11z}	2.93	1.93	1.83	1.63	1.63	1.62	1.36	1.32	1.20
v_{12z}	2.93	1.93	1.84	1.63	1.63	1.62	1.36	1.32	1.20

TABLE 3-2
MAGNITUDE ORDERING OF STEADY STATE SENSITIVITY COEFFICIENTS

$$\frac{\Delta x_i}{\Delta p_j}\bigg|_{t_f}$$

p_j \ x_i	ϕ_1	θ_1	ψ_1	ϕ_{35}	ψ_{24}	ψ_{35}	ω_{4x}	ω_{4z}	ω_{5z}	ω_{5x}	ϕ_{24}
c_{s35z}	3.28	2.39	1.49	1.11	1.07	1.07	-.641	-.578	-.578	-.546	-.502
c_{s24z}	3.28	2.39	1.49	1.11	1.07	1.07	-.641	-.578	-.578	-.546	-.502
c_{s13z}	2.93	2.06	1.33	.990	.952	.952	-.572	-.516	-.516	-.487	-.448
c_{s12z}	2.93	2.13	1.33	.990	.952	.952	-.572	-.516	-.516	-.487	-.448
v_{11z}	2.41	1.72	1.09	.812	.781	.781	-.469	-.423	-.423	-.400	-.368
v_{12z}	-2.40	-1.72	-1.09	-.812	-.781	-.781	.470	.423	.423	.400	.368

The same ordering applies to the six largest steady state
sensitivity ratios in the first column of entries of Table
3-2.

Although the detailed ordering of the sensitivity coeffi-
cients differs between the two tables beyond this point, cer-
tain common patterns may be discerned. The changes in model
parameters to which the state variables are most sensitive
are, in descending order, changes in the z axis damping coef-
ficients, c_{s35z}, c_{s24z}, c_{s13z}, c_{s12z}, and changes in the z
axis components of the location vectors of the hinges con-
necting body 1 to the adjacent bodies, v_{11z} and v_{12z}. In
addition, among the seven scalar state variables showing the
highest sensitivity to model parameter changes in both ta-
bles, six, the inertially referenced angular displacements of
body 1, ϕ_1, θ_1 and ψ_1, and the relative angular displacements
between the bodies close to the free ends of the appendages,
ψ_{24}, ψ_{35} and ϕ_{35}, are common to both although they appear
with different ordering.

3.4 REFERENCES

3-1 Chichester, F.D., "Application of Gauss-Siedel Multilevel Control to a Single Axis Torsional Model", <u>Proceedings of the Space Transportation Symposium,</u> 1980 SAE Aerospace Congress and Exposition, October, 1980, Los Angeles Convention Center, Los Angeles, CA.

3-2 Chichester, F.D., "Application of Gauss-Seidel Multilevel and LQR Control to a Three Axis Rotational Model of a Flexible Space Vehicle", <u>Proceedings of the Twelfth Annual Pittsburgh Conference on Modeling and Simulation,</u> April 1981., University of Pittsburgh, Pittsburgh, Pennsylvania, pp 1309-1315.

3-3 Chichester, F.D. and M.T. Borelli, "A Multilevel Control Approach for a Modular Structured Space Platform", <u>AGARDograph On Spacecraft Pointing and Position Control,</u> No. 260, November, 1981, Paper No. 10.

3-4 Chichester, F.D. "Development of a Three Axis Gauss-Siedel Multilevel Rotational Model of a Flexible Space Vehicle", <u>Proceedings of the Twelfth Annual Pittsburgh Conference on Modeling and Simulation,</u> April 1981, University of Pittsburgh, Pittsburgh, Pennsylvania, pp. 1303-1308.

SECTION 4

4.0 EVALUATING SOFTWARE CHANGES REQUIRED TO ACCOMMODATE ADDITION OF ANOTHER RIGID BODY TO AN EXISTING DISCRETE MASS MODEL OF A FLEXIBLE SPACECRAFT UNDER MODULAR ATTITUDE CONTROL.

4.1 INTRODUCTION

Earlier analyses of linearized state variable models of the rotational dynamics of flexible spacecraft under modular attitude control were predicated upon models comprised of a constant number of flexibly interconnected rigid bodies as in Chichester (4-1), 4-2), (4-3) and (4-4). However, situations can be anticipated in which it would be necessary to add one or more rigid bodies of appreciable weight to a flexible spacecraft while it is in orbit. This could occur, for example, in docking one spacecraft to another. For this reason, it was deemed desirable to evaluate systematically the changes in a representative flexible spacecraft model that would result from adding another rigid body to it. Furthermore, an attempt was to be made to recast the model of the flexible spacecraft into a form that would experience minimal changes due to the addition of a rigid body.

4.2 PARTITIONING OF ATTITUDE CONTROL PROBLEM FOR FIVE BODY MODEL

1. The linearized state variable model of rotational dynamics of the three axis five body approximation of the prototype flexible spacecraft depicted in Figure 2-1 was partitioned according to spatial axis and the y axis submodel was found to be decoupled from the submodel for the x and z axes.

4-1

2. The state vectors of each of the submodels of Step 1 was partitioned into a rigid body angular rate vector and an Euler angle vector for each spatial axis.

3. Each of the three spatial body angular rate vectors and the three spatial Euler angle vectors of Step 2 was partitioned into components corresponding to the five rigid bodies comprising the model. The resulting pair of partitioned submodels was written in the following form.

xz axes submodel:

$$\dot{\underline{x}}_1 = A_1 \underline{x}_1 + B_1 \underline{u}_1 \tag{4-1}$$

y axis submodel:

$$\dot{\underline{x}}_2 = A_2 \underline{x}_2 + B_2 \underline{u}_2 \tag{4-2}$$

where:

$$\underline{x}_1 = (\underline{\omega}_x^T, \underline{\phi}^T, \underline{\omega}_z^T, \underline{\psi}^T)^T = \text{xz axes state vector} \tag{4-3}$$

$$\underline{x}_2 = (\underline{\omega}_y^T, \underline{\theta}^T)^T = \text{y axis state vector} \tag{4-4}$$

$$\underline{u}_1 = (\underline{u}_x^T, \underline{u}_z^T)^T = \text{xz axes control vector} \tag{4-5}$$

$$\underline{u}_2 = \underline{u}_y = \text{y axis control vector} \tag{4-6}$$

$$\begin{aligned}
\underline{\omega}_x &= (\omega_{1x}, \omega_{2x}, \ldots, \omega_{5x})^T \\
\underline{\omega}_z &= (\omega_{1z}, \omega_{2z}, \ldots, \omega_{5z})^T \\
\underline{\omega}_y &= (\omega_{1y}, \omega_{2y}, \ldots, \omega_{5y})^T
\end{aligned} \tag{4-7}$$

$$\begin{aligned}
\underline{\phi} &= (\phi_{24}, \phi_{35}, \phi_{12}, \phi_{13}, \phi_1)^T \\
\underline{\psi} &= (\psi_{24}, \psi_{35}, \psi_{12}, \psi_{13}, \psi_1)^T \\
\underline{\theta} &= (\theta_{24}, \theta_{35}, \theta_{12}, \theta_{13}, \theta_1)^T
\end{aligned} \tag{4-8}$$

$$\underline{u}_x = (u_{1x},\ u_{2x},\ \ldots,\ u_{rx})^T;\ r \leq 5$$
$$\underline{u}_z = (u_{1z},\ u_{2z},\ \ldots,\ u_{rz})^T;\ r \leq 5 \qquad (4\text{-}9)$$
$$\underline{u}_y = (u_{1y},\ u_{2y},\ \ldots,\ u_{ry})^T;\ r \leq 5$$

A_1 = xz axes state vector coefficient matrix of dimensions 20 x 20 for 5 body model.

A_2 = y axis state vector coefficient matrix of dimensions 10 x 10 for 5 body model.

B_1 = xz axes control vector coefficient matrix of dimensions 20 x r for 5 body model.

B_2 = y axis control vector coefficient matrix of dimensions 10 x r for 5 body model.

4. The optimal attitude control subproblem associated with jth submodel (j = 1, 2) was written as follows:

Minimize:

$$P_j = \tfrac{1}{2} \int_{t_o}^{t_f} \left[(\underline{x}_j - \underline{x}_{jd})^T Q_j (\underline{x}_j - \underline{x}_{jd}) + \underline{u}_j^T W_{ju}\underline{u}_j \right] dt \qquad (4\text{-}10)$$

subject to:

$$\dot{\underline{x}}_j = A_j \underline{x}_j + B_j \underline{u}_j \qquad (4\text{-}11)$$

where:

    $\underline{x}_j$ = jth state vector

    $\underline{x}_{jd}$ = jth desired state vector

$\underline{u}_j$ = jth control vector

Q_j = jth state vector error weighting coefficient matrix

W_{ju} = jth control energy weighting coefficient matrix

t_O = initial time

t_f = final time

5. Application of linear quadratic regulator (LQR) techniques presented in Chichester (4-5) reduced each of the optimal attitude control subproblems to the solution of Riccati equations of the following form.

$$\dot{K}_j = -(K_j A_j + A_j^T K_j + K_j R K_j + Q_j) \quad j = 1, 2 \quad (4-12)$$

where:

$$R_j = -B_j W_{ju}^{-1} B_j^T \quad (4-13)$$

$$K_j(t_f) = [0] \quad (4-14)$$

For $j = 1$, the 5 body xz axes subproblem K_j is a 20 x 20 symmetric matrix; for $j = 2$, the 5 body y axis subproblem K_j is a 10 x 10 symmetric matrix.

4.3 PARTITIONING OF THE SIX BODY MODEL ATTITUDE CONTROL PROBLEM

The preceding steps were applied to the linearized state variable model of the rotational dynamics of the six body configuration depicted in Figure 4-1.

The state variable model for the six body configuration was written with the same structural form as that shown for the
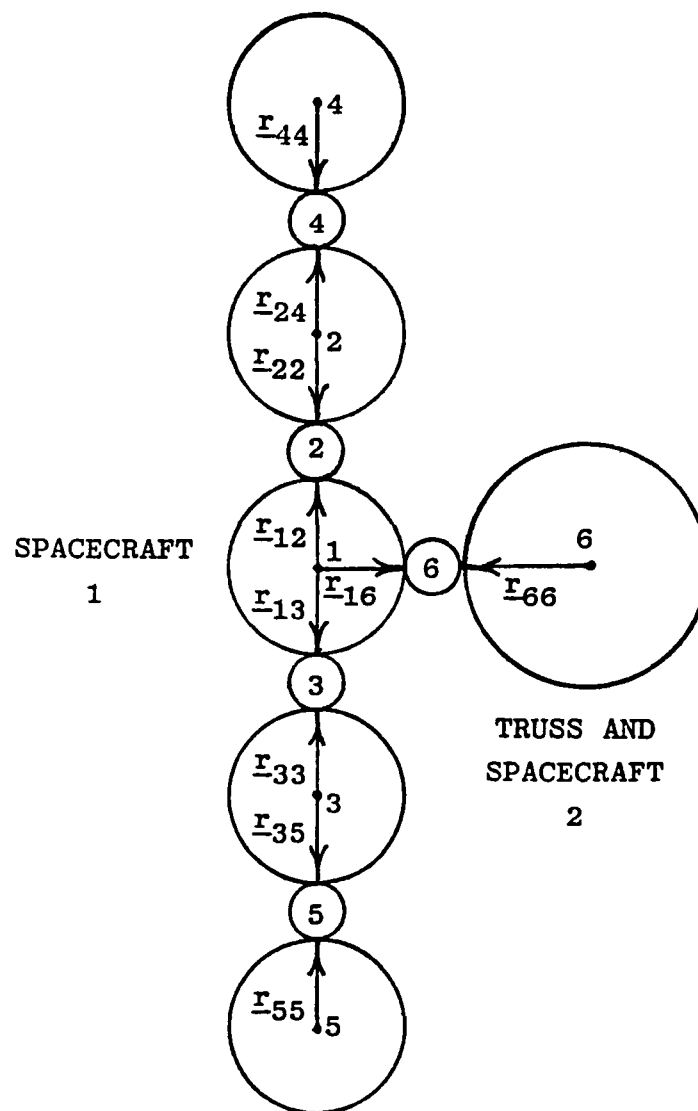
FIGURE 4-1

TOPOLOGICAL DIAGRAM OF SIX BODY MODEL

OF TWO SPACECRAFT INTERCONNECTED BY A DEPLOYABLE TRUSS

five body configuration in equations (4-1) and (4-2) with the connection of body 6 to body 1 being accommodated by incrementing the dimension of the state subvectors, $\underline{\omega}_x$, $\underline{\omega}_z$, $\underline{\omega}_y$, $\underline{\phi}$, $\underline{\psi}$ and $\underline{\theta}$, and the maximum allowable dimension, r, of the control vectors $\underline{u}_x$, $\underline{u}_z$ and $\underline{u}_y$, by one as follows.

$$\underline{\omega}_x = (\omega_{1x},\ \omega_{2x},\ \ldots,\ \omega_{5x},\ \omega_{6x})^T$$
$$\underline{\omega}_z = (\omega_{1z},\ \omega_{2z},\ \ldots,\ \omega_{5z},\ \omega_{6z})^T \qquad (4\text{-}15)$$
$$\underline{\omega}_y = (\omega_{1y},\ \omega_{2y},\ \ldots,\ \omega_{5y},\ \omega_{6y})^T$$

$$\underline{\phi} = (\phi_{24},\ \phi_{35},\ \phi_{12},\ \phi_{13},\ \phi_{1},\ \phi_{16})^T$$
$$\underline{\psi} = (\psi_{24},\ \psi_{35},\ \psi_{12},\ \psi_{13},\ \psi_{1},\ \psi_{16})^T \qquad (4\text{-}16)$$
$$\underline{\theta} = (\theta_{24},\ \theta_{35},\ \theta_{12},\ \theta_{13},\ \theta_{1},\ \theta_{16})^T$$

$$\underline{u}_x = (u_{1x},\ u_{2x},\ \ldots,\ u_{rx})^T;\ r \le 6$$
$$\underline{u}_z = (u_{1z},\ u_{2z},\ \ldots,\ u_{rz})^T;\ r \le 6 \qquad (4\text{-}17)$$
$$\underline{u}_y = (u_{1y},\ u_{2y},\ \ldots,\ u_{ry})^T;\ r \le 6$$

The rigid body angular rate subvectors of equation set (4-15) and the Euler angle subvectors of equation set (4-16) were aggregated into an xz axes submodel state vector and a y axis submodel state vector for the six body model of the same form as that displayed for the five body model in equations (4-3) and (4-4) and the control subvectors of equation set (4-17) were aggregated into an xz axes submodel control subvector and a y axis submodel control vector of the form shown for the five body model in equations (4-5) and (4-6).

4.4 COMPARISON OF PARTITIONED FIVE BODY AND SIX BODY ATTITUDE CONTROL PROBLEMS

1. The five body and six body xz axes and y axis submodels were partitioned in the manner suggested by equations (4-3) through (4-6) and compared as shown in the following equations.

Partitioned Five and Six Body xz Axes Submodels:

$$
\begin{bmatrix}
\dot{\underline{\omega}}_x \\
\dot{\underline{\phi}} \\
\dot{\underline{\omega}}_z \\
\dot{\underline{\psi}}
\end{bmatrix}
=
\underbrace{
\begin{bmatrix}
A_{11} & A_{12} & A_{13} & A_{14} \\
A_{21} & [0] & [0] & [0] \\
A_{31} & A_{32} & A_{33} & A_{34} \\
[0] & [0] & A_{43} & [0]
\end{bmatrix}
}_{A_1}
\begin{bmatrix}
\underline{\omega}_x \\
\underline{\phi} \\
\underline{\omega}_z \\
\underline{\psi}
\end{bmatrix}
$$

$$+ \, B_1 \underline{u}_1 \qquad\qquad (4\text{-}18)$$

Partitioned Five and Six Body y Axis Submodels:

$$
\begin{bmatrix} \dot{\underline{\omega}}_y \\ \hline \dot{\underline{\theta}} \end{bmatrix}
=
\underbrace{\begin{bmatrix} A_{55} & A_{56} \\ \hline A_{65} & [0] \end{bmatrix}}_{A_2}
\begin{bmatrix} \underline{\omega}_y \\ \hline \underline{\theta} \end{bmatrix}
+ B_2 \underline{u}_2
\qquad (4\text{-}19)
$$

where:

$$
B_1 = \begin{bmatrix} B_{11} & B_{12} \\ 0 & 0 \\ B_{31} & B_{32} \\ 0 & 0 \end{bmatrix}
$$

$$
B_2 = \begin{bmatrix} B_{51} \\ \hline 0 \end{bmatrix}
$$

A_{ij} = n x n state subvector coefficient submatrices for n body model (n = 5, 6)

[0] = n x n null submatrices

B_{ij} = n x r control subvector coefficient submatrices

0 = n x r null submatrices

Solid lines denote boundaries of submatrices of 6 body model.

Dashed lines denote locations of rows and columns added due to addition of 6th body.

From equations (4-18) and (4-19) it is evident that addition of body 6:

a. added four new rows and four new columns to the state vector coefficient matrix of the xz axes submodel;

b. added four new rows and increased the upper bound on the number of columns of the control vector coefficient matrix of the xz axes submodel by two;

c. added two new rows and two new columns to the state vector coefficient matrix of the y axis submodel;

d. added two new rows and increased the upper bound on the number of columns of the control vector coefficient matrix of the y axis submodel by one.

2. Algebraic expansions of the submatrices revealed that elements of the state vector coefficient matrices of the xz axes and y axis submodels of the five body configuration were affected by the addition of body 6 as follows.

   a. Null elements remained null elements implying that null submatrices remain null submatrices.

   b. Elements lying in the columns and rows associated with the body to which body 6 was attached experienced much larger changes in magnitude than the remaining elements.

3. From equations (4-3) and (4-4), (4-12) through (4-14) and equations (4-18) and (4-19) it was seen that addition of body 6 increased the dimensions of K_1, the solution of the Riccati equation associated with the xz axes submodel, from 20 x 20 to 24 x 24 and the dimensions of K_2, the solution of the Riccati equation associated with the y axis submodel, from 10 x 10 to 12 x 12.

4.5 REVIEW OF ALTERNATE PARTITIONINGS

1. The xz axes submodel was decomposed into an x axis submodel and a z axis submodel to replace the solution for the K_1 Riccati matrix of dimension 24 x 24 by the sequential solution for the Riccati matrix, K_x, of dimension 12 x 12 for the x axis submodel and the Riccati matrix, K_z, of dimension 12 x 12 for the z axis submodel of the six body configuration.

2. Additional decompositions of the xz axes submodel and the y axis submodel were developed analytically.

4.6 REFERENCES

4-1 Chichester, F.D. "Development of a Three Axis Gauss-Siedel Multilevel Rotational Model of a Flexible Space Vehicle", <u>Proceedings of the Twelfth Annual Pittsburgh Conference on Modeling and Simulation</u>, April 1981, University of Pittsburgh, Pittsburgh, Pennsylvania, pp. 1303-1308.

4-2 Chichester, F.D., "Application of Gauss-Seidel Multilevel and LQR Control to a Three Axis Rotational Model of a Flexible Space Vehicle", <u>Proceedings of the Twelfth Annual Pittsburgh Conference on Modeling and Simulation,</u> April 1981, University of Pittsburgh, Pittsburgh, Pennsylvania, pp 1309-1315.

4-3 Chichester, F.D. "Modeling Rotational Dynamics of a Flexible Space Platform for Application of Multilevel Attitude Control", <u>Proceedings of the 1982 American Control Conference,</u> June 1982, Arlington, Virginia, pp. 636-642.

4-4 Chichester, F.D. and M.T. Borelli, "A Multilevel Control Approach for a Modular Structured Space Platform", <u>AGARDograph On Spacecraft Pointing and Position Control,</u> No. 260, November, 1981, Paper No. 10.

4-5 Chichester, F.D., "Modular Design Attitude Control System", Final Report, NASA Contract No. NAS 8-33979 for George C. Marshall Space Flight Center, March 8, 1982.

SECTION 5

5.0 COMPARING ATTITUDE CONTROL EFFECTIVENESS FOR ACTUATORS ON TWO BODIES OF THE MODEL WITH THAT FOR ACTUATORS RESTRICTED TO A SINGLE BODY OF THE SAME MODEL

5.1 INTRODUCTION

The digital computer simulations of the five body approximation of the prototype flexible spacecraft under modular attitude control reported in Chichester (5-1) and Tiffany (5-2) were predicated upon restriction of the control actuators to the central body (body 1) of the model. This restriction reflected the fact that control torques should not be applied directly to the lightweight solar wings or panels approximated by the remaining four rigid bodies and the flexible suspension connecting them to the central body. However, the addition of a sixth rigid body and its associated hinge characteristics producing the six body configuration, shown in Figure 4-1, introduced the possibility, if not the necessity, of placing actuators on both bodies 1 and 6 in order to effect attitude control of the resulting vehicle. The possible need for the addition of actuators on body 6 arose from the fact that this appendage, representing a combination of a second spacecraft and the deployable truss connecting it to the five body model of the prototype flexible spacecraft, involved much higher concentrations of mass and rotational inertias than did the two appendages representing the solar wings (bodies 2,4 and bodies 3,5). Two principal questions to be addressed in this study were the following:

1. Would the modular control system have enough authority to control the six body model's attitude effectively if the actuators were restricted to the central body?

2. Would the addition of actuators to body 6 improve the effectiveness of the modular attitude control significantly without generating excessive coupling effects between the actuators on bodies 1 and 6?

5.2 PROCEDURE FOLLOWED

1. Numerical values of the physical parameters of rigid body 6 and three degree of freedom hinge 6 of the six body configuration depicted in Figure 4-1 were chosen so that the oscillatory modes of this single body and hinge would closely match the lowest oscillatory modes of the assembly of bodies and hinges representing the truss and spacecraft 2 in the ten body configuration shown in Figure 2-2.

    a. The location of the center of mass and the principal moments of inertia about this center of mass were determined for the five serially connected bodies representing the truss and spacecraft 2.

    b. A two body model consisting of the single body model of the truss attached in cantilever fashion to a wall of very high mass and inertia was developed.

    c. Equations were developed for calculating the spring coefficients for the three degree of freedom hinge between the bodies of the two body model as a function of the natural frequencies of the undamped model of this configuration and its rotational inertia coefficients.

    d. Equations were developed for calculating the damping coefficient corresponding to n% damping for each

spring coefficient associated with the joint in the two body model of the truss as cantilever.

e. The natural frequencies associated with the lowest oscillatory mode about each spatial axis in the five body model of the four body representation of the truss attached to a wall were equated with the natural frequencies of the two body cantilever model.

2. The xz axis submodel, equation (4-18), and the y axis submodel, equation (4-19), of the six body configuration were modified for restriction of actuators to body 1 and also to bodies 1 and 6.

   a) Restriction of the actuators to the central body (body 1) reduced the control subvectors, $\underline{u}_x$, $\underline{u}_z$ and $\underline{u}_y$ to u_{1x}, u_{1z} and u_{1y}, respectively, and the B_{ij} and 0 submatrices to the dimensions 6 x 1.

   b) Corresponding to restriction of the actuators to bodies 1 and 6 the control subvectors were truncated to:

   $$\underline{u}_x = (u_{1x}, \ u_{6x})^T;$$

   $$\underline{u}_y = (u_{1y}, \ u_{6y})^T;$$

   $$\underline{u}_z = (u_{1z}, \ u_{6z})^T.$$

   The second through fifth columns were then removed from the B_{ij} and 0 submatrices reducing their dimensions to 6 x 2.

3. The xz axes submodel and the y axis submodel for the six body configuration were simulated on the digital computer for restriction of actuators to body 1 and for restric-

tion of actuators to bodies 1 and 6 under modular attitude control.

4. Initial angular displacements of .5 degrees with respect to each spatial axis were applied to the central body (body 1) and at each of the three degree of freedom hinges between the rigid bodies of the model and the resulting responses were plotted and tabulated.

5.3   RESULTS

The maximum magnitudes of the Euler angles of the rigid bodies comprising the xz axis submodel with selected distributions of actuators and sensors are listed in Tables 5-1 and 5-2. Since the magnitude of each initial angular displacement was .5 degrees, entries in the tables of substantially greater magnitude imply considerable overshoot in the responses. Each row of either table represents the maximum magnitudes of the Euler angles of a spatial axis for the set of conditions listed at the left side. The angles with subscript "1" are the inertially referenced attitude angles of the central body (body 1). The double subscripts identify the interface with which the corresponding Euler angle is associated (ϕ_{12} refers to the angle about the x axis between bodies 1 and 2). The angle labels at the top of the table are arranged in approximate spatial order as depicted in Figure 4-1.

From these tables the following were observed.

1. The largest maximum Euler angle magnitudes for a given set of conditions generally occur at the outer extremities of the solar panels.

TABLE 5-1

X AXIS MAXIMUM EULER ANGLE RESPONSES FOR
DIFFERENT DISTRIBUTIONS OF ACTUATORS AND SENSORS

	$\left|\phi_{35}\right|_{max}$ [deg.]	$\left|\phi_{13}\right|_{max}$ [deg.]	$\left|\phi_{1}\right|_{max}$ [deg.]	$\left|\phi_{16}\right|_{max}$ [deg.]	$\left|\phi_{12}\right|_{max}$ [deg.]	$\left|\phi_{24}\right|_{max}$ [deg.]
Actuators and Position Sensors on Bodies 1 & 6 ψ_{24} & ψ_{35} Sensors	1.16	.50	.612	.50	.50	1.12
Actuators and Sensors on Body 1 ψ_{24} & ψ_{35} Sensors with Body 6 Sensors	1.18	.50	.627	.758	.50	1.13
Actuators and Position Sensors on Bodies 1 & 6 ψ_{24} & ψ_{35} Sensors with Asymmetric Displacements	1.24	.50	.50	.514	.50	1.55

TABLE 5-2

Z AXIS MAXIMUM EULER ANGLE RESPONSES FOR
DIFFERENT DISTRIBUTIONS OF ACTUATORS AND SENSORS

	$\left\lvert\psi_{35}\right\rvert_{max}$ [deg.]	$\left\lvert\upsilon_{13}\right\rvert_{max}$ [deg.]	$\left\lvert\psi_{1}\right\rvert_{max}$ [deg.]	$\left\lvert\psi_{16}\right\rvert_{max}$ [deg.]	$\left\lvert\psi_{12}\right\rvert_{max}$ [deg.]	$\left\lvert\psi_{24}\right\rvert_{max}$ [deg.]
Actuators and Position Sensors on Bodies 1 & 6 ψ_{24} & ψ_{35} Sensors	.849	.50	.688	.572	.50	.849
Actuators and Position Sensors on Body 1 ψ_{24} & ψ_{35} Sensors with Body 6 Sensors	.856	.50	.725	.732	.50	.856
Actuators and Position Sensors on Bodies 1 & 6 ψ_{24} & ψ_{35} Sensors with Asymmetric Displacements	1.10	.50	.507	.50	.50	1.12

2. Elimination of the control actuators from body 6, one of the two bodies on which they can be placed, increases the overshoot in the responses of the central body (body 1) and the responses of the relative Euler angles between bodies 1 and 6 to the point where they are very poorly controlled.

3. Application of asymmetric initial displacements in the Euler angles at the three degree of freedom hinges between the rigid bodies of the model produced Euler angle responses with especially high overshoots close to the outer extremities of the solar panels.

Responses of the relative Euler angle between bodies 1 and 6 for the y axis submodel with selected distributions of actuators and sensors are presented in Figures 5-1 and 5-2. Since this submodel is linear, the responses actually are sinusoidal in nature although, in some instantances, the characteristics of the plotting subroutine utilized may result in their appearing to be comprised of contiguous straight line segments.

From Figures 5-1 and 5-2, the following were observed.

1. Elimination of control actuators from one of the two bodies on which they could be placed, body 6, introduces an offset in the final or steady state value of the responses of the relative Euler angle between bodies 1 and 6.

2. Elimination of control actuators from body 6 renders control of the relative Euler angle between bodies 1 and 6 completely ineffectual about the y axis even with sensors present on body 6 which was seen by comparing Figure 5-2 with Figure 5-1.
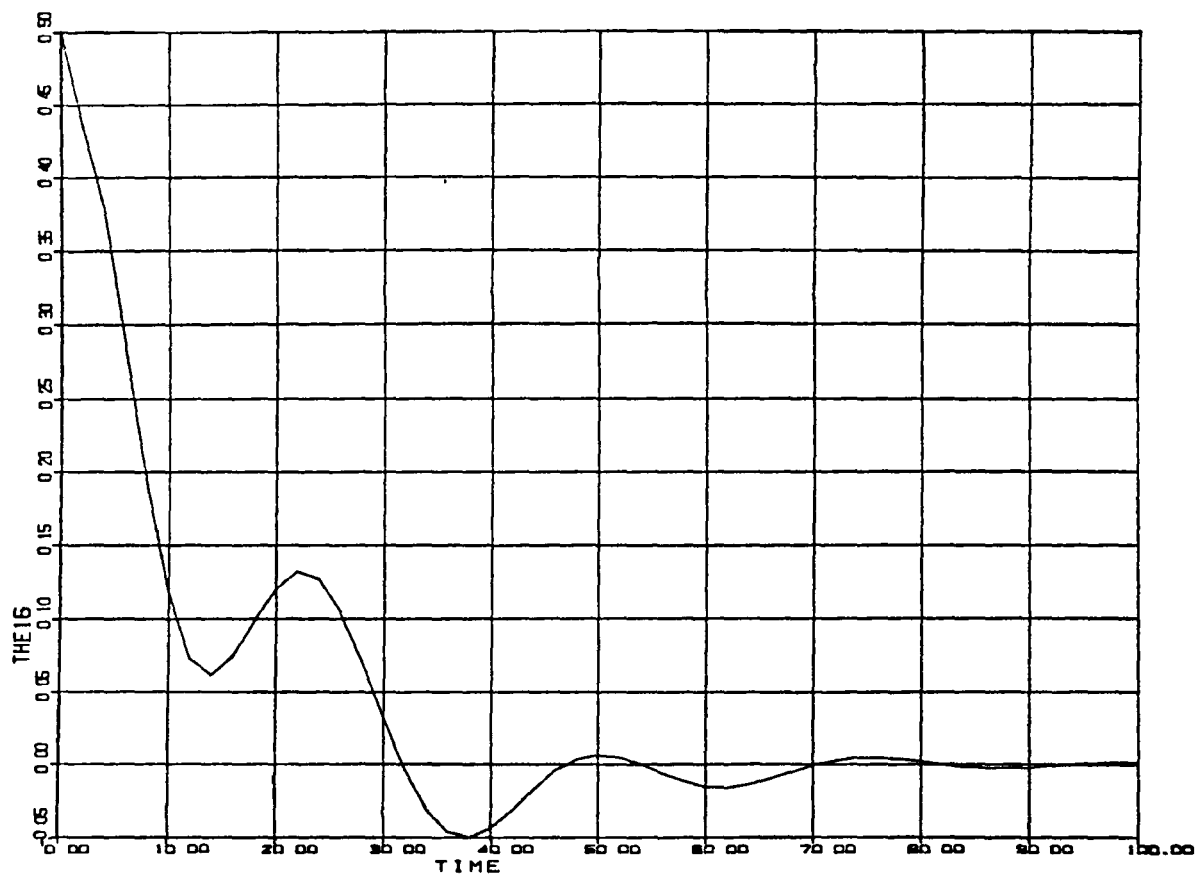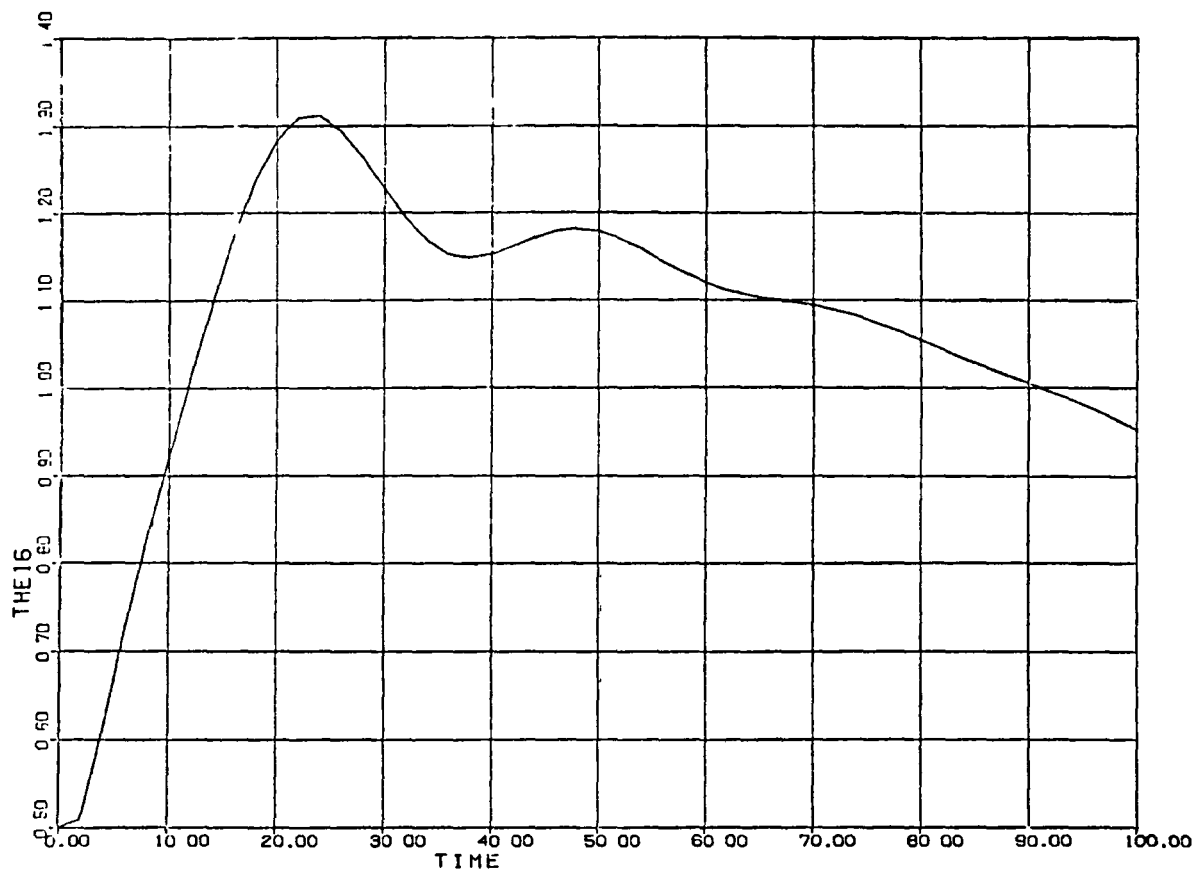
FIGURE 5-1

θ_{16} RESPONSE TO SYMMETRIC INITIAL
EULER ANGULAR DISPLACEMENTS WITH ACTUATORS AND
RATE SENSORS ON BODIES 1 AND 6 AND ψ_{24}, ψ_{35} SENSORS

5-8

FIGURE 5-2

θ_{16} RESPONSE TO SYMMETRIC INITIAL
EULER ANGULAR DISPLACEMENTS WITH ACTUATORS ON BODY 1,
RATE SENSORS ON BODIES 1 AND 6 AND ψ_{24}, ψ_{35} SENSORS

5-9

5.4   REFERENCES

5-1 Chichester, F.D., "Application of Gauss-Seidel Multilevel
     and LQR Control to a Three Axis Rotational Model of a
     Flexible Space Vehicle", <u>Proceedings of the Twelfth An-
     nual Pittsburgh Conference on Modeling and Simulation,</u>
     April 1981., University of Pittsburgh, Pittsburgh, Penn-
     sylvania, pp 1309-1315.

5-2 Tiffany, N.O., "Multilevel Control by Partitioning",
     Bendix Engineering Development Center Internal
     Memorandum, April 14, 1981.

SECTION 6

6.0 CONCLUSIONS AND RECOMMENDATIONS

During the period covered by this report the digital computer
simulation of the ten body approximation of the three axis
rotational dynamics model of a prototype flexible space plat-
form consisting of two spacecraft interconnected by the
MSFC/hybrid deployable truss with modular control was accom-
plished except for the completion of validation runs. An
important part of this task was the generation of numerical
values of the physical parameters of a five body approxima-
tion of the three axis rotational dynamics of the MSFC/hybrid
truss in cantilever configuration that matched five modes of
the dynamic responses of this approximate model with those of
a finite element NASTRAN model of the truss that was sup-
plied.

The remainder of the effort during this time period utilized
a five body approximation of a three axes model of the rota-
tional dynamics of a prototype flexible spacecraft and a six
body approximation of the ten body model of the flexible
space platform described above. The five body model was
utilized to evaluate the effects of elimination of state
variable sensors upon the modular attitude control of the
prototype flexible spacecraft and to generate sensitivity
coefficients of its state variables with respect to the mod-
el's parameters. The six body model was used to evaluate
software changes required to accommodate the addition of
another body to the five body model and to compare the effec-
tiveness of attitude control for actuators on two of the
model's bodies with that when the actuators were restricted
to a single body of the same model.

6.1 CONCLUSIONS

The following conclusions are based mainly upon modeling and digital computer simulation of a four body approximation of the three spatial axes rotational dynamics of the MSFC/hybrid deployable truss, modeling simulation and control of a five body approximation of a prototype flexible spacecraft and modeling, simulation and control of a six body approximation of the space platform which consists of two spacecraft interconnected by the MSFC/hybrid deployable truss.

1. Five modes of the rotational dynamics of a three dimensional finite element NASTRAN model of the MSFC/hybrid deployable truss were closely approximated by matching the eigenvalues of a four body model of the truss with those of the NASTRAN model.

2. The close approximation of the dynamic modes of the NASTRAN model of the truss by those of the four body model supported the incorporation of the latter model in the ten body model representing two spacecraft interconnected by the MSFC/hybrid deployable truss.

3. Due to the light damping present in the vehicle model, it was difficult to control oscillations at the free ends of the appendages with control actuators restricted to the central body.

4. Increasing the magnitude of the elements in the diagonal weighting matrix, W_u, for the control vector in the quadratic performance index tended to decrease the amount of control torque expended about a given axis but it also reduced the effectiveness of attitude control about that axis.

5. Increasing the magnitude of the elements in the diagonal weighting matrix, Q, for the state vector in the quadratic performance index tended to decrease the peak magnitude of the corresponding state variable but it also reduced the effectiveness of the attitude control about the corresponding axis.

6. The changes in parameter values of the five body model to which the scalar state variables (axial components of body angular rates and Euler attitude angles of the rigid bodies in the model) are most sensitive, are in descending order, changes in the z axis damping coefficients, c_{s35z}, c_{s24z}, c_{s13z}, c_{s12z}, and changes in the z axis components of the location vectors of the hinges connecting the central body (body 1) to the adjacent bodies, v_{11z}, and v_{12z}.

7. Among the seven scalar state variables of the five body model showing the highest peak sensitivity and the seven state variables showing the highest steady state sensitivity, six parameters are common to both groups.

8. The computer software developed for the five body model may be extended to accommodate the addition of another body if provisions are made for the expansions in the dimensions of the subvectors and submatrices of the partitioned form of the model described in equations (5-18) and (5-19) and for the changes in the values of the elements of the matrices, especially those associated with the rows and columns corresponding to the rigid body to which the sixth body is attached. These concepts also may be applied to the case in which another body is added to the ten body model of the space platform.

9. For the six body approximation of a flexible space plat-
   form, depicted in Figure 5-1:

   a. Control actuators and sensors must be present on <u>both</u>
      bodies 1 and 6 and sensors of relative Euler angular
      displacements about the z axis close to the extremi-
      ties of the solar panels are required for effective
      three axis attitude control of the spacecraft in re-
      sponse to symmetric initial angular displacements.

   b. Elimination of the control actuators from body 6 left
      insufficient control authority for effective attitude
      control even with the appropriate sensors on body 6.

6.2   RECOMMENDATIONS

The following items are recommended for future study concern-
ing control of flexible spacecraft.

1. The effects of incomplete state feedback upon the atti-
   tude control of the five body model of the prototype
   flexible spacecraft should be investigated.

2. The partitioning applied to the five body state variable
   model of the flexible spacecraft should be extended to
   the Riccati equations associated with the corresponding
   optimal attitude control problem.

3. A prototype sigle axis model of a flexible spacecraft
   should be developed to facilitiate comparison of differ-
   ent attitude control approaches with minimal computer
   requirements.

4. Procedures should be developed for estimating the real time computational requirements for the controlled spacecraft models.

5. The attitude responses of the flexible spacecraft models with modular control should be compared with those obtained for the same models with classical frequency domain control to determine those conditions under which modular control might be advantageous.

6. A control concept consisting of determination of the number of control moment gyros, determination of a control law and design of a mission operations momentum management plan should be developed for at least one representative spacecraft.

7. Methods of momentum management for counteracting the bias portion of the external torques on the space vehicle should be developed.

8. A momentum management algorithm should be developed under which a spacecraft automatically adjusts its attitude with respect to the orbit plane in such a way as to minimize the angular momentum buildup.

End of Document